JOURNAL OF MATERIALS SCIENCE 21 (1986) 583–590

Structural studies on γ-MnO_2 by transmission electron microscopy

PIERRE STROBEL, JEAN-CLAUDE JOUBERT
Laboratoire de Cristallographie CNRS, associé à l'USMG, 166X – 38042 Grenoble Cedex, France

MARIA-JESUS RODRIGUEZ
Departmento de Química Inorgánica, Facultad Químicas, Universitad Complutense, Madrid-3, Spain

Single-crystal electron diffraction patterns were obtained on five specimens of γ-MnO_2: one natural, two electrolytical (EMD) and two chemical (CMD) samples. EMDs are best described by the orthorhombic structure proposed by De Wolff which is derived from the ramsdellite structure. A CMD prepared from $MnCO_3$ fits the hexagonal cell of "ε-MnO_2". Flaky grains from the natural sample and fibres from a CMD prepared from $Mn(NO_3)_2$ are hexagonal with a new cell: $a \simeq 0.494$, $c \simeq 0.539$ nm. No simple relation between chemical composition, morphology and structure could be found.

1. Introduction

The structure of γ-MnO_2, the non-stoichiometric form of manganese dioxide widely used in the battery industry, has long been a subject of controversy [1–5]. X-ray diffraction does not give conclusive information, since the diffraction lines are few and mostly broad. No single crystals of this material have ever been synthesized. Three kinds of crystallographic indexing of the powder X-ray patterns have been proposed: an orthorhombic cell A with $a = 0.445$, $b = 0.935$, $c = 0.285$ nm [1, 4], a hexagonal cell B with $a = 0.280$, $c = 0.445$ nm [5], and an alternate hexagonal cell C with $a = 0.965$, $c = 0.442$ nm [6]. The A cell results from the description of γ-MnO_2 as an intergrowth of blocks of two crystalline forms of manganese dioxide, pyrolusite (or β-MnO_2) and ramsdellite. Its parameters can vary considerably with the OH content (b values from 0.930 to 1.070 nm have been reported [7, 8]). A variant A′ with axes $a' = b/2$, $b' = 2a$, $c' = c$ has also been suggested [9]. The B cell is based on a hexagonal packing of oxygen atoms with random occupancy of half the octahedral sites by manganese atoms. It has been considered by some authors as a different form of manganese dioxide, ε-MnO_2 [2, 5], in spite of the extreme similarity of ε- and γ-MnO_2 X-ray powder patterns [2, 10].

Chemically, γ-MnO_2 samples are usually distinguished by their preparation method, which consists of either electrolytical oxidation of Mn^{2+} or aqueous redox chemistry (giving the so-called "electrolytical" or "chemical" manganese dioxide, EMD or CMD, respectively). There is no conclusive evidence of structural or electrochemical difference between EMDs and CMDs.

More structural information could be obtained by transmission electron microscopy (TEM), which explores microscopic domains instead of the macroscopic, average structure. Difficulties arise, however, if the material is sensitive to heat or radiation damage, as has been observed on γ-MnO_2 [1], or if the crystallites are very small. Giovanoli *et al.* [1], observed electron diffraction on a cooled specimen of CMD; their results are consistent with De Wolff's intergrowth model (cell A). More recently, Turner and Buseck [11] examined three natural samples of γ-MnO_2 by high-resolution TEM, which revealed a more complicated intergrowth structure than De Wolff's (with three different kinds of building units containing tunnels 1×1 (as in β-MnO_2), 2×1 (as in ramsdellite) and also 3×1).

The scarcity of accurate structural data and the possible correlations between structure and electrode behaviour prompted us to examine various specimens of γ-MnO_2 of both EMD and CMD types by TEM. It will be shown that the actual symmetry of the crystallites can be unambiguously determined by electron diffraction, and that variations in chemical preparation or in morphology are not connected with any significant structural changes.

2. Experimental techniques

2.1. Preparation

In addition to seven industrial specimens (see sources in Table I), two CMD samples were prepared following the synthesis procedures of Parida *et al.* [12]: calcination of freshly precipitated $MnCO_3$ at 673 K in air followed by leaching for 2 h in 3M HNO_3 at 363 K (Sample 9), or treating $Mn(OH)_2$ freshly precipitated at pH 9 to 9.5 for 2 h in cold 3M HNO_3 (Sample 11). Both samples were dried in air at 373 K for one week.

2.2. Characterization

X-ray powder diffraction patterns were taken in a Guinier–Hägg camera with Fe$K\alpha$ radiation ($\lambda =$

0022–2461/86 $03.00 + .12

TABLE I Origin and physicochemical characteristics of γ-MnO_2 samples

Sample No.	Origin	Mn, (wt %) w	Mn oxidation state, z	OH fraction, x*	H_2O fraction, y*	Morphology	Electron diffraction patterns
1	Natural mineral	48.2	3.871	0.129	1.495	flakes and columns	single crystal
2	EMD from $MnSO_4$ (Hoechst, GFR)	57.0	3.961	0.039	0.52	flakes and isolated needles	single crystal
3	CMD from Mn acet. (Sedema, Belgium)	60.6	3.876	0.124	0.20	flakes	–
4	"Thermal" (dec. $Mn(NO_3)_2$)	55.4	3.929	0.071	0.675	very thin fibres (1 single flake)	from groups of crystals
5	Industrial EMD (Japan)	59.7	3.871	0.129	0.275	very small flakes	powder diffraction
6	Industrial CMD (Wonder, France)	59.3	3.913	0.087	0.31	small flakes	powder and some crystals
7	Industrial EMD (Tekkosha, Greece)	59.0	3.946	0.054	0.34	flakes and columns	single crystal
9	CMD, as sample 9 in [12]	60.6	3.869	0.131	0.20	crystallized elongated flakes	single crystal
11	CMD as Sample 11 in [12]	58.6	3.679	0.321	0.36	very small elongated flakes	– (powder diffraction after annealing)

*Assuming the formula $MnO_{2-x}(OH)_x \cdot yH_2O$.

0.193 73 nm). Samples were analysed for total manganese content (by atomic absorption spectrophotometry) and for active oxygen (by the oxalate method [13]).

2.3. Electron microscopy

Specimens for electron microscopy were ground in acetone in an agate mortar and deposited on a copper grid covered with a thin holey carbon film. They were examined in a Philips EM400T electron microscope fitted with a double-tilt side-entry goniometer and operating at 120 kV.

3. Results

3.1. Macroscopic characterization of samples

3.1.1. Chemical composition

The total manganese content w (wt %) and its average oxidation state z in each sample are given in Table I. Assuming the formula $MnO_{2-x}(OH)_x$, yH_2O, analytical results give x values in the range 0.04 to 0.13, except for Sample 11, which contains more (OH) groups, i.e. more Mn^{3+}. The natural sample 1 has a particularly low manganese content, corresponding to a high water fraction, but possibly also to the presence of impurities (anionic and cationic). The water content y varies with the drying procedure. Annealing Samples 7 and 9 at 473 K for 24 h, for example, resulted in mass losses of 2.0 and 2.3 wt %, corresponding to 30.4 and 57.9% of the water, respectively.

3.1.2. X-ray diffraction

All samples exhibit the few typical d-spacings of γ-MnO_2, especially the broad lines around 0.241, 0.213 and 0.163 nm. The broad line at $d \simeq 400$ pm reported by most authors (ascribed to (1 1 0) in the orthorhombic cell A, but not indexable in the hexagonal cell B) was not observed in Guinier patterns. Samples 3 and 11 gave very weak patterns even after extended exposure, indicating either poor crystallinity or very small grain size. Sample 1 is exceptional again: it shows numerous sharp lines which cannot be fitted to any of the proposed γ-MnO_2 cells (d = 0.428, 0.3345, 0.3035, 0.2281 and 0.2094 nm). A possible cause for these diffraction lines is the inclusion of minor foreign phases, as is common in natural minerals. Sample 5 shows a sharp line at d = 0.3116 nm; this line can be indexed with cell A as (0 3 0) (usually not observed), but comes more probably from traces of β-MnO_2, of which it is the strongest line (1 1 0).

3.2. Morphology

The morphology of various samples investigated is shown in Figs. 1a to e. Most specimens consist of flaky grains with rounded edges (see for example Figs. 1b, d). In several cases (Samples 1, 2 and 7), flakes are accompanied by isolated columnar crystals (Figs. 1a, b).

Two specimens have particular morphologies: Sample 4, which is *fibrous* (Fig. 1c), and Sample 9 ("homemade" CMD), which contains well-crystallized, bean-shaped grains (Fig. 1e). Whenever possible, electron diffraction patterns were recorded on both "columnar" and "flaky" grains of a grain specimen. The grain size was particularly small in samples 3, 5, 6, 11 (two CMDs and two EMDs) (Fig. 1d).

3.3. Electron diffraction

Samples 3 and 11, already noted for their very weak X-ray patterns, gave no observable electron diffraction, indicating poor crystallization. Samples 5 and 6 (both industrial EMDs) contained too small grains for recording electron diffraction patterns from isolated single crystals. Powder rings were observed, together with some rows of single-crystal reflections with d-spacings $\simeq 0.310$ nm (Fig. 2). This interplanar distance is not specific for γ-MnO_2: it occurs in γ-MnO_2 with cell A, in β-MnO_2 and in α-MnO_2 (but not in γ-MnO_2 with the hexagonal cell B). The rings correspond to the typical intense reflections of γ-MnO_2 (see Table II). Similar diffraction rings were obtained on Sample 11

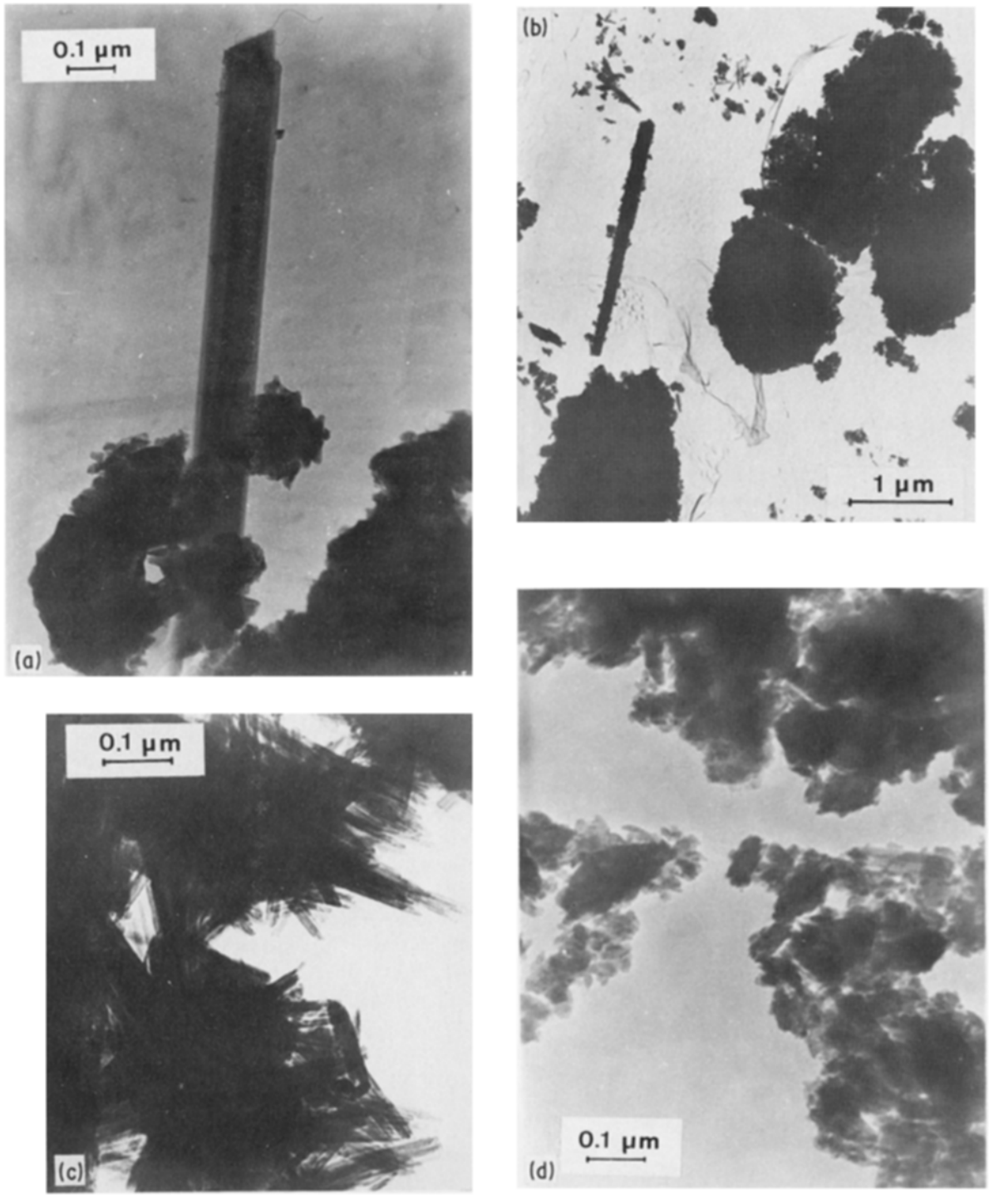

Figure 1 Typical morphology of "γ-MnO_2" samples: (a) Sample 1, (b) Sample 2, (c) Sample 4, (d) Sample 6, (e) Sample 9.

after annealing for 8 days at 573 K (the $d = 0.31$ nm ring was also observed on this specimen).

Four grains from Sample 1 were found suitable for electron diffraction, and no less than three different structures were found among them. The columnar crystal shown in Fig. 1a yielded diffraction patterns, which could be indexed at best with the hollandite-type structure (see Fig. 3); it consists therefore of α-MnO_2, instead of the expected γ-MnO_2. Flakes from Sample 1 gave two kinds of diffraction patterns. Those shown in Fig. 4 are well described by the A cell (orthorhombic), which is typical of γ-MnO_2 [1, 4]. (Such patterns cannot be satisfactorily indexed with the hexagonal cells B or C.) Those shown in Fig. 5, obtained on another flake from Sample 1, are incompatible with any of the crystallographic cells mentioned above. Rotation about the horizontal axis in Figs. 5a to c allowed a determination of a hexagonal cell with $a \simeq 0.49$, $c \simeq 0.53$ nm.

Samples 2 and 7 gave clear diffraction patterns, which are exactly similar to those in Fig. 4. These samples (both EMDs) are therefore orthorhombic γ-MnO_2. On the other hand, Sample 4 gave electron diffraction patterns corresponding exactly to the new hexagonal cell found in Sample 1, although these two samples exhibit very different morphologies. Additional reciprocal planes of the new lattice were recorded on Sample 4 (see Fig. 5d).

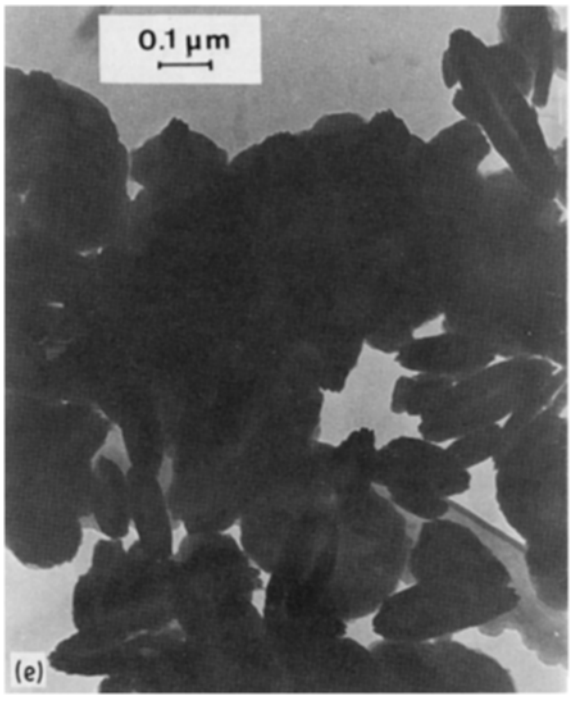

Figure 1 Continued.

Two crystallites of Sample 9 were examined. They are clearly hexagonal (see [0 0 1] zone, Fig. 6a). Rotation about [1 0 0]* (Fig. 6a to d) shows that Sample 9 corresponds to the B cell (hexagonal, $a \simeq 0.280$, $c \simeq 0.445$ nm ("ε-MnO_2"). The c/a value calculated from five electron diffraction patterns is 1.60 (1), in good agreement with ε-MnO_2 cell data.

During the examination of Sample 9, which was kept under the electron beam for several hours, a significant decrease in d-spacing values was found in $(0\,k\,2)$* planes. This is probably an example of a chemical reaction of the specimen under electron irradiation, leading to a composition shift within the sample (in the case of the orthorhombic structure, a continuous composition range from MnO_2 to MnOOH is known to exist [7, 8]).

4. Discussion

4.1. Morphology

Many authors have attempted to establish a relationship between the morphology of γ-MnO_2 and its structure or chemical reactivity. As early as 1950, Brenet *et al.* [14] had suggested that "battery-active" MnO_2 is characterized by an acicular morphology. Ghosh and Brenet [15] found both "rounded particles" and needles in industrial Japanese EMD, the latter being considered as MnOOH resulting from cell discharge. The acicular morphology has been later associated with the ε-MnO_2 hexagonal form [5, 16].

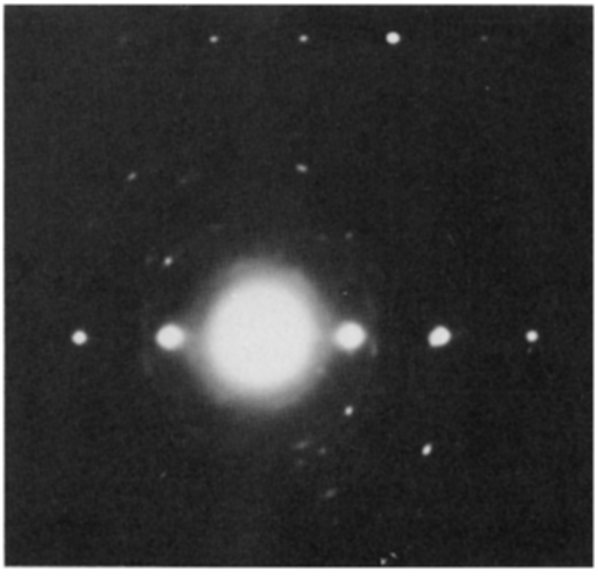

Figure 2 Electron diffraction pattern of Sample 6 (CMD), showing diffraction rings and dots.

Morphological differences may be actually misleading. In todorokite, another disordered manganese oxide, electron microscopy revealed that a wide variation in morphology (from fibrous to platey) is possible due to twinning [17]. In γ-MnO_2, Giovanoli *et al.* [3] have shown that (i) a "fibrous" EMD observed under high resolution consists of very small flaky crystals very similar to those in the usual EMDs [3], (ii) round grains of CMD can be partially recrystallized into needle shape with no noticeable structural change [3]. The most striking result of the present study is the similarity of the structures of flakes from Sample 1 and fibres from Sample 4. Only Sample 9 (ε-MnO_2) has a particular morphology (bean-like, rounded-edge grains), possibly related to a particular structure; its morphology, however, differs from that reported earlier [5, 16] for ε-MnO_2.

4.2. Crystal structure

From the crystallographic point of view, our results bring little clarification about the actual crystallographic description of γ-MnO_2. We listed in Section 1 four proposed cells A, A′, B, C. The A cell was observed in Samples 1 (natural mineral), 2 and 7 (EMDs); it is the cell closely related to that of ramsdellite and α-MnOOH (groutite). A′ and C did not fit the observed diffraction patterns.

TABLE II Indexation of significant d-spacings in various cells

d (nm)	β-MnO_2 rutile	α-MnO_2 hollandite	γ-MnO_2/ramsdellite (orthorhombic A cell)	ε-MnO_2 (hexagonal B cell)	New hexagonal cell
0.400*	–	–	1 1 0	–	–
0.286†	0 0 1	0 0 1	0 0 1	–	–
0.240*	–	2 1 1	0 2 1	1 0 0	1 1 0
0.213*	1 1 1	(≃ 3 1 0)	1 2 1	1 0 1	2 0 0
0.163*	2 1 1	4 3 1, 5 0 1	2 2 1	1 0 2	1 0 3, 2 1 0

*Typical "γ-MnO_2" line.
†Typical rutile-like chain line.

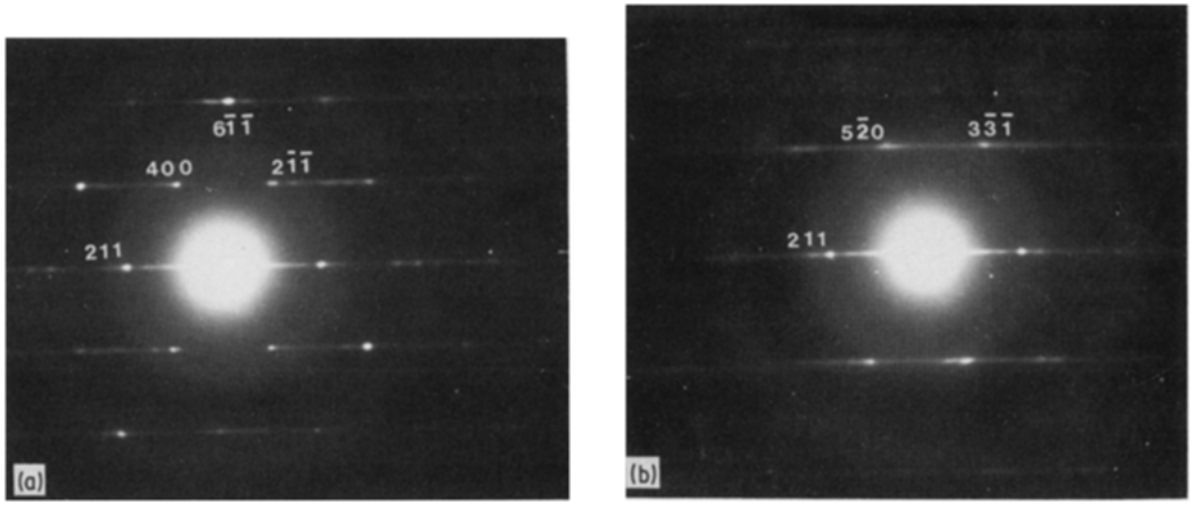

Figure 3 Electron diffraction patterns from a columnar crystal of Sample 1 (see Fig. 1a): α-MnO_2, hollandite-type structure. Rotation about [2 1 1]*.

Sample 9 (a CMD) clearly corresponds to ε-MnO_2 (B-cell). Note that this phase was obtained previously only by electrolysis under specific synthesis conditions [5], while we prepared it chemically. Peculiar features were observed on several of the diffraction patterns from Sample 9: (i) weak spots at $h\,1\,\frac{1}{2}$ in the [0 $\bar{1}$ 2] zone (see arrows in Fig. 6b), (ii) diffuse lines parallel to [1 0 0]* in [0 1 $\bar{1}$] and [0 2 $\bar{1}$] zones (Figs. 6c and d). These lines can be seen as the intersections of a particular diffusion plane with the successive diffraction planes (see Fig. 7). It follows that this reciprocal diffusion plane is (0 0 1)*.

Both effects can be explained in view of the structural model proposed by De Wolff *et al.* [5] to describe the ε-MnO_2 structure: this model consists of a hexagonal compact framework of oxygen atoms in which half the octahedral sites are randomly occupied by manganese atoms. In the *h c c* lattice, octahedral sites are stacked parallel to the *c*-axis, forming chains of face-sharing octahedra. This leads to short Mn–Mn distances and strong repulsions if adjacent sites are occupied. The weak spots (i), which correspond to a doubling of *c*, mean that the occupation of the octahedral sites by mangenese atoms in rows along *c* is not statistical, but partially ordered from row to row. Moreover, Mn^{4+} cations in a given row are likely to be shifted apart along *c* by electrostatic repulsion when two adjacent sites occur to be occupied. On average, manganese positions are distributed over a range of *z*-coordinates, giving rise to the reciprocal diffusion plane (0 0 1)*. Note that the resolution of the diffusion line into discrete spots is improved by annealing (compare Figs. 6c and e), which means that the annealed sample is more ordered.

Another particular effect is visible in Fig. 6b, where satellite spots occur around (*h* 2 1) reflections. Their meaning is not clear; they resemble figures caused by double diffraction in the presence of a second crystal [19], but do not appear on all reflections (they are absent on (*h* 0 0) spots).

Finally, a new hexagonal cell had to be introduced. It is compatible, as well as the hexagonal ε-MnO_2 cell, with the typical *d*-spacings of "γ-MnO_2" (see Table II). (The line at $d \simeq 400$ nm is not indexable, but it is not observed systematically in Guinier patterns.) The new structure was found in two different samples in this study: the natural mineral (Sample 1) and the "MnO_2" obtained by low-temperature decomposition

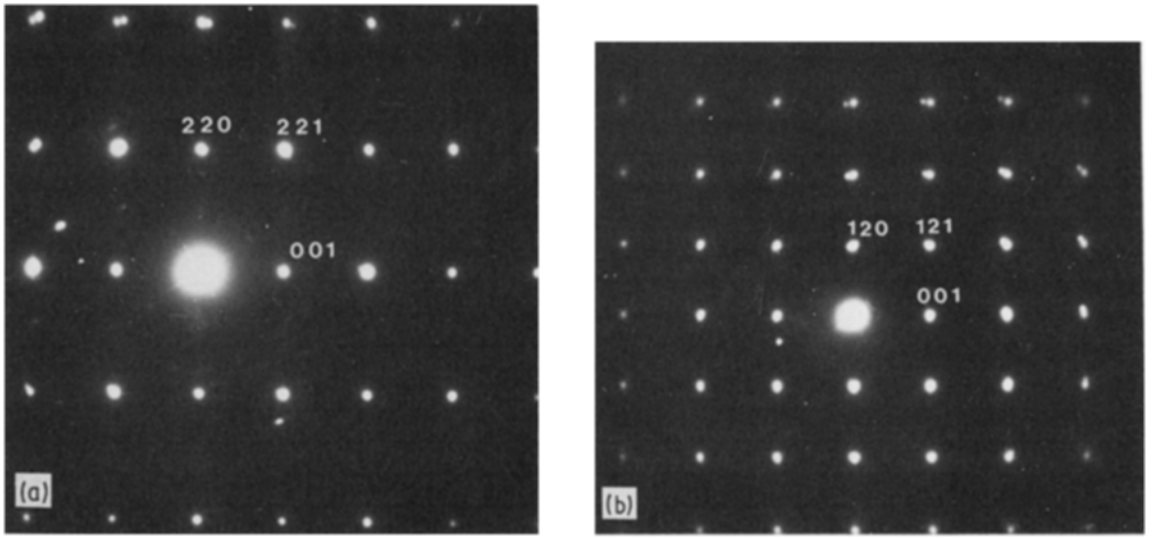

Figure 4 Electron diffraction patterns from a flake of Sample 1: orthorhombic structure (A cell), rotation about [0 0 1]*.

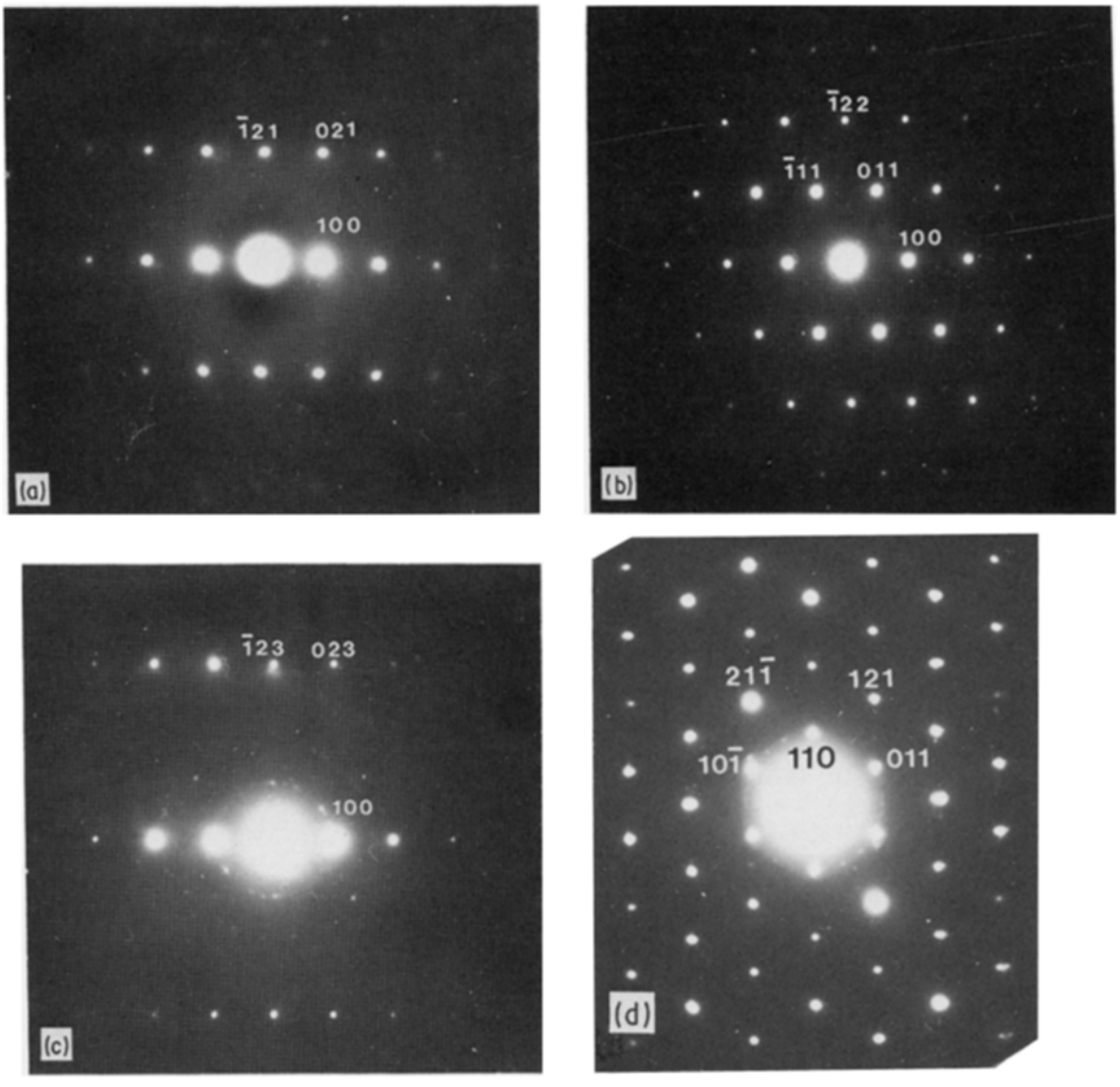

Figure 5 Electron diffraction patterns corresponding to a new hexagonal cell with $a \simeq 0.494$, $c \simeq 539$ nm. (a) to (c) rotation about [1 0 0]* ([0 k $\bar{2}$] zones); (d) [1 $\bar{1}$ 1] zone, showing the [1 1 0]* axis. Patterns recorded on Samples 1 (b), (c) and 4 (a), (d).

of manganese nitrate (Sample 4). It should be noted that this structure accounts for several of the foreign X-ray diffraction lines observed in the Guinier pattern of Sample 1, particularly those at $d = 0.428$, 0.3344 and 0.2287 nm, indexed as 1 0 0, 1 0 1 and 1 0 2, respectively. The cell parameters deduced from the Guinier pattern are: $a = 0.494(2)$ nm, $c = 0.539(2)$ nm.

There is an important structural difference between both hexagonal cells and the other structures of the "MnO_2" family: the absence of the translation at

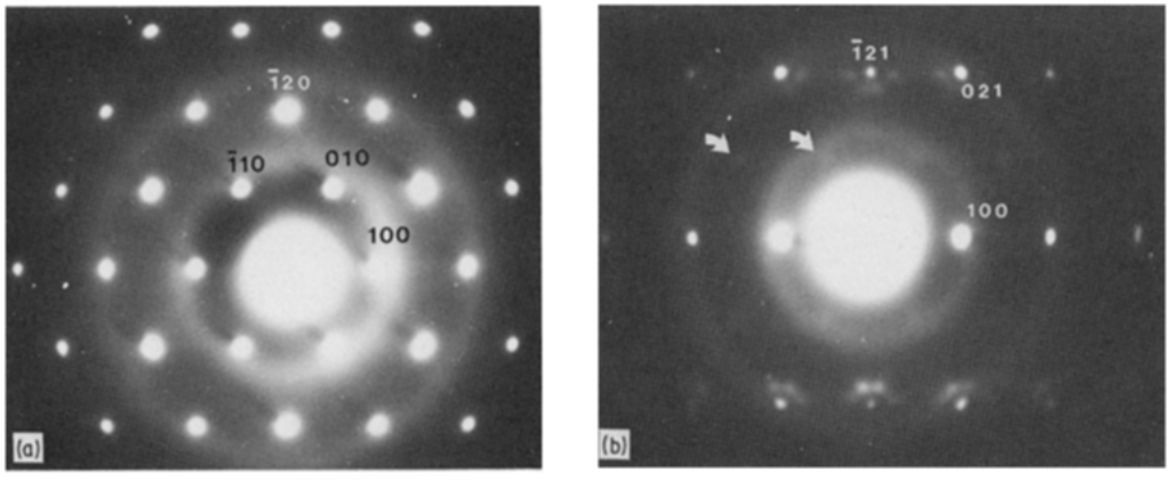

Figure 6 Electron diffraction patterns of Sample 9 (CMD): bean-shaped grains (see Fig. 1e). Hexagonal cell, ε-MnO_2 structure, rotation about [1 0 0]*. (e) Same orientation as (c), but annealed sample (8 days at 573 K). The rings (absent in e) are due to the carbon film. For arrows, see Section 4.2.

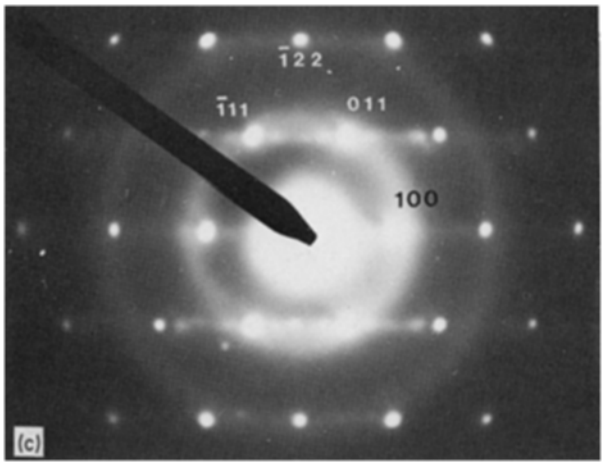

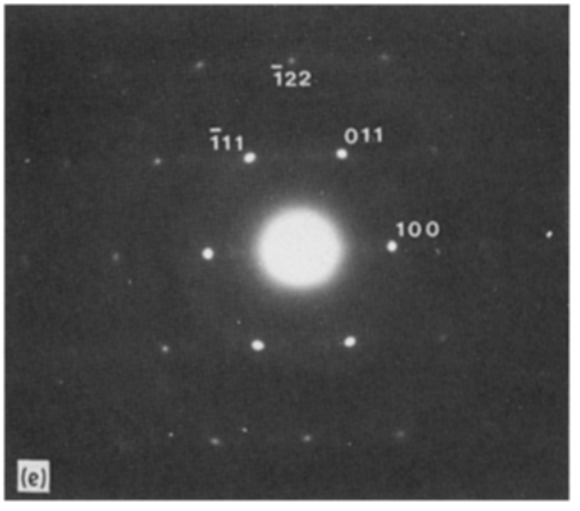

$d \simeq 0.286$ nm, which results from the presence in the structure of edge-sharing, rutile-like chains of octahedra as found in α-MnO_2 (hollandite), β-MnO_2 (pyrolusite) and in ramsdellite (see Table II).

Annealing, which was carried out on Samples 7, 9 and 11, improved the crystallinity of the compounds: Sample 11 diffracted significantly better after annealing (but gave only powder diffraction rings), while

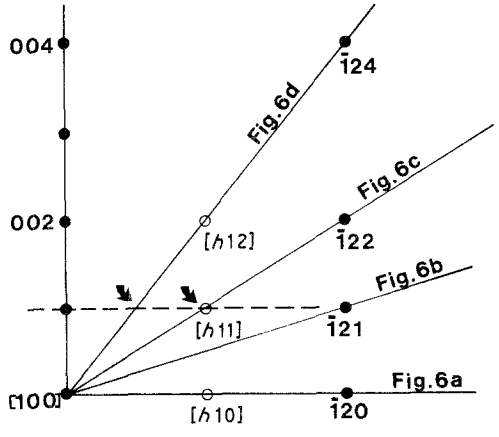

Figure 7 The diffusion plane (dotted line) shown with respect to the diffraction planes of Fig. 6. The rotation axis [1 0 0]* (horizontal axis in Fig. 6) is perpendicular to the plane of the paper; black circles show reflections in the plane of the figure; open circles show rows of reflections above and below the plane of the paper. The intersections of the diffusion plane with diffraction planes are indicated by arrows.

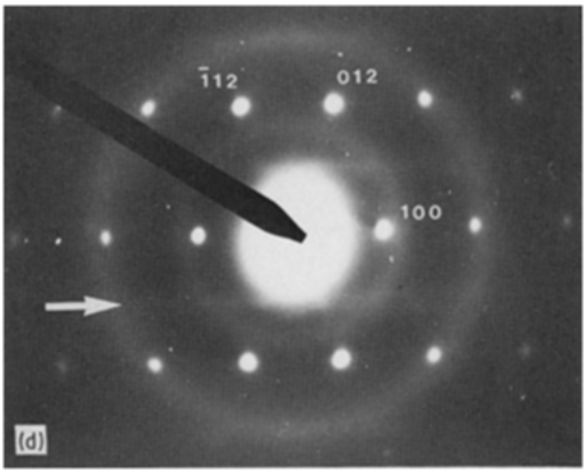

Figure 6 Continued.

annealed ε-MnO_2 (Sample 9) gave diffraction patterns showing evidence of better ordering of the manganese atoms than in the non-annealed specimen.

5. Conclusion

Nine different samples of γ-MnO_2 of various origins were studied by TEM. The crystallinity of five of them, while inadequate as expected for accurate X-ray studies, allowed us to record single-crystal electron diffraction patterns. EMDs are better described by the orthorhombic cell corresponding to De Wolff's structural model, while two distinct hexagonal structures were found: a partially ordered B cell ("ε-MnO_2") in Sample 9 (a CMD with typical round-edged grains), and a new hexagonal cell with $c/a = 1.08$, which describes crystals from Samples 1 (natural) and 4 ("thermal"). Apart from the Sample 9 case, apparent morphological differences are not simply connected to different structure types. We believe that grain size (which influences kinetics and sorption), chemical composition and structural defaults [11, 20] are parameters which are as important as crystal structure for battery activity.

Acknowledgements

The authors are indebted to all persons who made synthetic samples available to us, especially Dr F. Tedjar (Sétif University, Algeria). The help and advice of M. Alario-Franco (Universitad Complutense, Madrid, Spain) in electron microscopy, and of Mrs P. Amiot (Laboratoire des Basses Températures, C.N.R.S., Grenoble) in chemical analysis is gratefully acknowledged.

References

1. R. GIOVANOLI, R. MAURER and W. FEITKNECHT, *Helv. Chim. Acta* **50** (1967) 1072.
2. R. GIOVANOLI, MnO_2 Symposium Proceedings, edited by B. Schumm, H. M. Joseph and A. Kozawa (The Electrochemical Society, Cleveland, USA, 1980) p. 113.
3. R. GIOVANOLI, *Prog. Batteries and Solar Cells* **2** (1979) 116.
4. P. M. De WOLFF, *Acta Crystallogr.* **12** (1959) 341.
5. P. M. De WOLFF, J. W. VISSER, R. GIOVANOLI and R. BRÜTSCH, *Chimia* **32** (1978) 257.
6. G. M. FOULRING, *Amer. Mineral.* **50** (1965) 170.
7. W. FEITKNECHT, H. R. OSWALD and U.

FEITKNECHT-STEINMANN, *Helv Chim. Acta* **43** (1960) 1947.
8. W. C. MASKELL, J. E. A. SHAW and F. L. TYE, *Electrochim. Acta* **26** (1981) 1403.
9. F. FREUND, E. KÖNEN and E. PREISLER, MnO_2 Symposium Proceedings, edited by A. Kozawa and R. J. Brodd, (The Electrochemical Society, Cleveland, USA, 1975) p. 328.
10. K. J. EULER and R. KIRCHHOF, *Electrochim. Acta* **26** (1981) 1383 (see footnote, p. 1386).
11. S. TURNER and P. R. BUSEK, *Nature* **304** (1983) 143.
12. K. M. PARIDA, S. B. KANUNGO and B. R. SANT, *Electrochim. Acta* **26** (1981) 435.
13. D. A. PANTONY and A. SIDDIQI, *Talanta* **9** (1962) 811.
14. J. BRENET, H. FORESTIER and J. BOISSIER, Congrés de Microscopie Optique (Paris, 1950), *Rev. Opt. (Paris)* (1952) 297.
15. S. GHOSH and J. BRENET, *Electrochim. Acta* **7** (1962) 449.
16. L. PONS and J. BRENET, *C.R. Acad. Sci. (Paris)* **260** (1965) 2483.
17. S. TURNER and P. R. BUSECK, *Science* **212** (1981) 1024.
18. R. GIOVANOLI, W. FEITKNECHT and P. GEORGES, *Chimia* **30** (1976) 268.
19. P. HIRSCH, A. HOWIE, R. B. NICHOLSON, D. W. PASHLEY and M. J. WHEELAN, "Electron Microscopy of thin crystals," (Krieger, Malabar, USA, 1977) Ch. 6.4.
20. P. RUETSCHI, *J. Electrochem. Soc.* **131** (1984) 2737.

Received 15 November 1984
and accepted 29 March 1985